Langmuir

ARTICLE

pubs.acs.org/Langmuir

Single Kaolinite Nanometer Layers Prepared by an In Situ Polymerization−Exfoliation Process in the Presence of Ionic Liquids

Sadok Letaief,[†,‡] Jérôme Leclercq,[†] Yun Liu,[‡] and Christian Detellier*[,†,‡]

[†]Department of Chemistry and [‡]Center for Catalysis Research and Innovation, University of Ottawa, Ottawa ON, Canada K1N 6N5

Supporting Information

ABSTRACT: A simple chemical route for the exfoliation of kaolinite in the presence of polymerizable ionic liquids and the resulting obtainment of exfoliated nanocomposites is reported. The exfoliation was achieved using three different ionic liquids structurally bearing a vinyl group: 1-methyl-3-(4-vinylbenzyl)imidazolium chloride salt (IL_1), 1-methyl-1-(4-vinylbenzyl)pyrrolidinium chloride (IL_2), and 1-methyl-3-vinyl imidazolium iodide (IL_3) and a urea-kaolinite intercalate as precursor. The reaction was done in one step by an in situ polymerization−exfoliation process. ^{13}C CP/MAS NMR spectra confirmed the spontaneous polymerization of the ionic liquid during the exfoliation process to afford atactic polystyrene derivatives in the case of IL_1 and IL_2. The amount of organic material in the exfoliated nanocomposite was close to 30% as shown by thermal gravimetric analysis. This amount is small in comparison to the amount obtained when the exfoliation was done using sodium polyacrylate (Letaief and Detellier, *Langmuir* **2009**, *25*, 10975). XRD as well as SEM analysis confirmed a total exfoliation of the kaolinite when the reaction was done using urea kaolinite, whereas a microcomposite, made predominantly of kaolinite platelet aggregates dispersed in the polymeric matrix, was formed when dimethylsulfoxide kaolinite was used as the precursor.

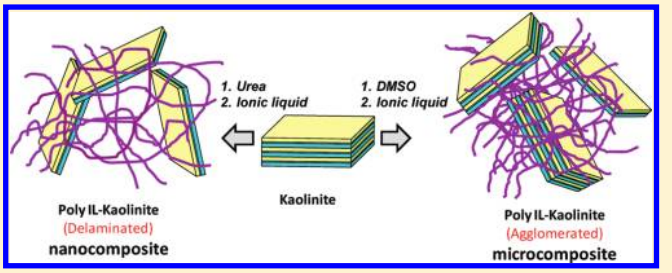

INTRODUCTION

The delamination or exfoliation of layered materials in a polymeric matrix leads to nanomaterials with improved properties compared to those of the starting inorganic and/or organic materials.[1] It was recently proposed by Bergaya et al.[2] that the term delamination designates the separation of adjacent layers, while the term exfoliation should be reserved for the limit case of complete loss of crystallographic orientation, layers becoming independent from one another.[2] Thus, exfoliated nanocomposites result from the loss of periodicity in the stacking of a layered inorganic material, giving rise to thin layers of less than 1 nm thickness randomly distributed in a polymeric matrix. These exfoliated compounds show potential for a wide range of applications in various fields: sensors,[3,4] biomedical engineering and pharmaceutical science,[5,6] catalysis,[7,8] electrical conductivity,[9−11] and separation membrane,[12−14] among others. The typical methodology for the exfoliation of layered materials consists, in a first step, of the intercalation between the individual layers of an organic polymer. The incorporation of a silica and titanium oxide network prepared by sol−gel transition from the hydrolysis of alkoxysilanes has also been reported.[15,16] A variety of layered inorganic materials have been used,[17] such as phosphates and phosphonates,[18] layered metal oxides,[19] layered double hydroxides,[20] layered polysilicates,[21] and clay minerals.[22] Among clay minerals, the smectite family has been widely studied,[15,23−29] but the number of reports of a chemical exfoliation of kaolinite is scarce.[30,31] The exfoliation of kaolinite to form nanotubes or nanoscrolls was also recently reported.[32] The rarity of kaolinite exfoliation is due to the remarkable structure of this mineral. Kaolinite is a 1:1 dioctahedral layered mineral whose layers are formed of siliceous tetrahedral sheets linked to aluminum octahedral sheets. The stacked layers are tightly bound together by van der Waals interactions and a network of hydrogen bonds.[33,34] This makes intercalation in the interlayer spaces of this mineral much more difficult than in the case of the swelling smectites.

A few examples of intercalated polymer−kaolinite nanocomposites have been reported. In these cases, the layered periodicity was maintained.[35−43] A new route for the exfoliation of kaolinite was reported recently. It was based on the grafting of an amino alcohol on the interlayer aluminol surfaces, followed by quaternarization using iodomethane, and then reaction of the resulting nanohybrid cationic polyelectrolyte with an organic anionic polyelectrolyte, sodium polyacrylate.[30] No reports have appeared so far on the exfoliation of kaolinite by in situ polymerization of an organic monomer.

In this work, a successful kaolinite exfoliation procedure was achieved using the intercalation of ionic liquid salts bearing a vinyl group: (i) 1-methyl-3-(4-vinylbenzyl)imidazolium chloride (IL_1), (ii) 1-methyl-1-(4-vinylbenzyl)pyrrolidinium chloride (IL_2), and (iii) 1-methyl-3-vinyl imidazolium iodide (IL_3). A urea kaolinite (Urea-K) intercalate was used as precursor. Their intercalation was concurrent with polymerization and

Received: September 5, 2011
Revised: November 6, 2011
Published: November 10, 2011

Scheme 1. Chemical Structure of the Three Ionic Liquids Used for the Exfoliation of Kaolinite

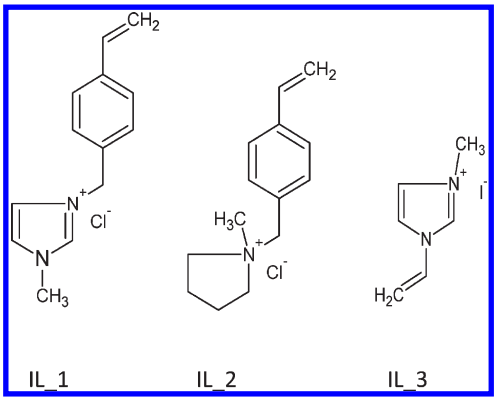

exfoliation. When dimethylsulfoxide kaolinite (DMSO-K) was used as the precursor, the exfoliation was incomplete.

The crucial point of difference between this work and the previously reported procedure[30] is that, in the present case, the reaction was done in one step by an in situ polymerization−exfoliation process, whereas in the case of the exfoliation with the sodium polyacrylate, kaolinite underwent two chemical modifications before the exfoliation process. XRD as well as SEM analysis confirmed a total exfoliation of kaolinite. The amount of the organic material found into the nanohybrid after exfoliation was close to 30%. This amount is small compared to the amount acquired when the exfoliation was done using sodium polyacrylate,[30] giving a nanocomposite with a high inorganic content.

Scheme 2. Exfoliation Procedure of Kaolinite Resulting from Ionic Liquid Polymerization, Using Urea-K or DMSO-K as Starting Material

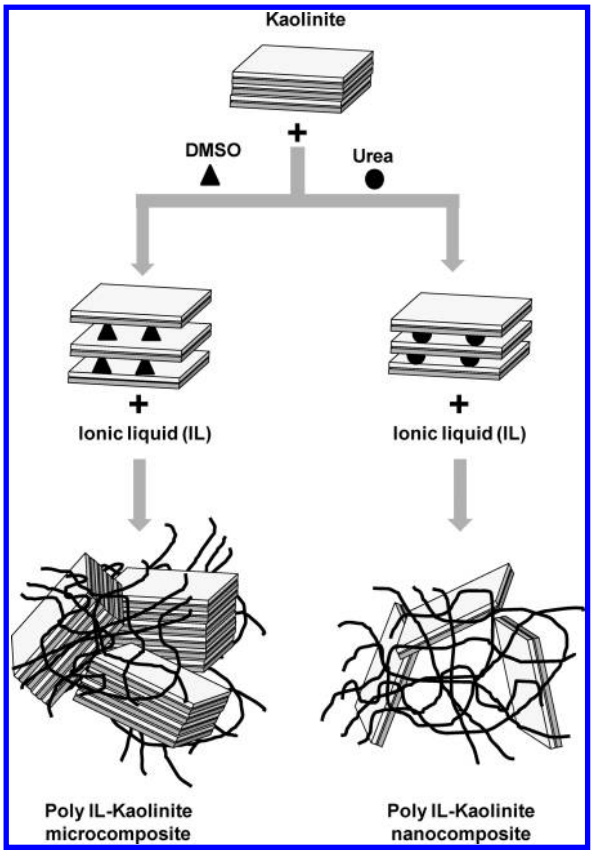

EXPERIMENTAL SECTION

Materials. Well-crystallized kaolinite (KGa-1b; Georgia) was obtained from the Source Clays Repository of the Clay Minerals Society, Purdue University, West Lafayette, IN, USA. The purification of KGa-1b and the preparation of Urea-K and DMSO-K intercalates were done according to previously published procedures.[44,45] DMSO, urea, 1-methylimidazole, 4-vinylbenzyl chloride, 1-methylpyrrolidone, iodomethane, and 1-vinylimidazole were purchased from Aldrich Chemicals and were used as received without further purification.

Sample Preparation. *Synthesis and Characterization of the Ionic Liquids IL_1, IL_2, and IL_3 (Scheme 1). IL_1.* The ionic liquid was synthesized using a variation of a published procedure.[46] 1-Methylimidazole (2.05 g, 25 mmol) and 4-vinylbenzyl chloride (4.6 g, 30 mmol) were added to 20 mL of dichloroethane. The mixture was refluxed overnight at 70 °C. The excess of 4-vinylbenzyl chloride was removed by washing with diethyl ether, and the resulting 1-methyl-3-(4-vinylbenzyl)imidazolium chloride salt was stored for further characterization and use. ^{1}H NMR (D_2O; ppm): δ 3.64 (s, 3 H, C***H***$_3$-N), 5.08 (d, 1 H, phenyl−CH=HC−***H***$_E$; J_{cis} = 10.6 Hz), 5.09 (s, 2 H, phenyl−C***H***$_2$−N), 5.57 (d, 1 H, phenyl−CH=***H***$_Z$C−H; J_{tr} = 17.3 Hz), 6.43 (dd, 1 H, phenyl−C***H***=HC−H), 7.13−7.22 (m, 6 H, ***phenyl*** ring and imidazole ring N−C**H**−C**H**−N), 8.60 (s, 1 H, imidazole ring N−C**H**−N). The ^{13}C NMR peaks attribution was made from empirical calculations and a 2D HSQC spectrum. See Figure 3 for annotation. ^{13}C NMR (D_2O; ppm): δ 35.9 (***C***H$_3$−N), 52.6 (phenyl−***C***H$_2$−N), 115.6 (phenyl−CH=***C***H$_2$), 122.2 and 124.0 (imidazole ring ***C***−***C***−N), 126.9 (phenyl *d*), 129.2 (phenyl *e*), 133.2 (phenyl *c*), 135.6 (phenyl *f* ; imidazole ring N−**C**−N), 138.2 (phenyl−**C**H=CH$_2$).

IL_2. The synthetic procedure was applied as in the case of IL_1, using 1-methylpyrrolidine instead of 1-methylimidazole. 1-Methylpyrrolidine (2.13 g, 25 mmol) and 4-vinylbenzyl chloride (4.6 g, 30 mmol) were added to 20 mL of dichloroethane. The mixture was refluxed overnight at 70 °C. The excess of 4-vinylbenzyl chloride was removed by washing with diethyl ether, and the resulting 1-methyl-3-(4-vinylbenzyl)pyrrolidinium chloride salt was stored for further characterization and use. ^{1}H NMR (D_2O; ppm): δ 2.07 (m, 4 H, −C***H***$_2$−CH$_2$−N−CH$_2$−C***H***$_2$−), 2.75 (s, 3 H, C***H***$_3$−N), 3.3 (m, 4 H, −C***H***$_2$−C***H***$_2$−N−C***H***$_2$−CH$_2$−), 4.3 (s, 2 H, phenyl−C***H***$_2$−N), 5.26 (d, 1 H, phenyl−CH=HC−***H***), 5.78 (d, 1 H, phenyl−CH=***H***C−H), 6.61(m, 1 H, phenyl−C***H***=HC−H), 7.3−7.5 (m, 4 H, ***phenyl*** ring). ^{13}C NMR (D_2O; ppm): δ 20.9 (−***C***H$_2$−CH$_2$−N−CH$_2$−***C***H$_2$−), 47.6 (***C***H$_3$−N), 63.3 (−CH$_2$−***C***H$_2$−N−***C***H$_2$−CH$_2$−), 66.1 (phenyl−***C***H$_2$−N), 116.3 (phenyl−CH=***C***H$_2$), 126.7−139.4 (***phenyl*** ring and phenyl−***C***H=CH$_2$).

IL_3. 1-Vinylimidazole (2.35 g, 25 mmol) was added to 20 mL of dichloroethane. Then, 4.26 g of iodomethane (30 mmol) was added dropwise to the mixture at room temperature. The mixture was stirred for 24 h at room temperature, and the excess of iodomethane was removed by washing with diethyl ether. The resulting 1-methyl-3-vinyl imidazolium iodide salt was stored for further characterization and use. ^{1}H NMR (D_2O; ppm): δ 3.83 (s, 3 H, C***H***$_3$−N), 5.31 (d, 1 H, N−CH=HC−***H***), 5.70 (d, 1 H, N−CH=***H***C−H), 7.02 (m, 1 H, N−C***H***=HC−H), 5.57 (d, 1 H, phenyl−CH=***H***C−H), 6.43 (m, 1 H, phenyl−C***H***=HC−H), 7.41 and 7.64 (imidazole ring N−C**H**−C**H**−N). ^{13}C NMR (D_2O; ppm): δ 36.1 (***C***H$_3$−N), 109.3 (N−CH=***C***H$_2$), 119.3 (N−***C***H=CH$_2$), 124.0 (imidazole ring ***C***−***C***−N), 128.4 (imidazole ring N−**C**−N).

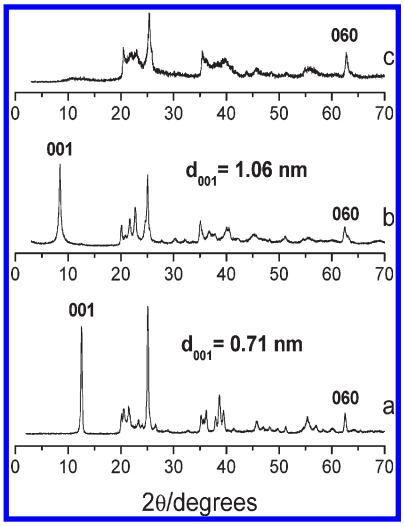

Figure 1. Powder XRD patterns (2θ = 2−70°) of (a) kaolinite; (b) Urea-K, and (c) the exfoliated nanocomposite obtained after reaction of Urea-K with IL_1.

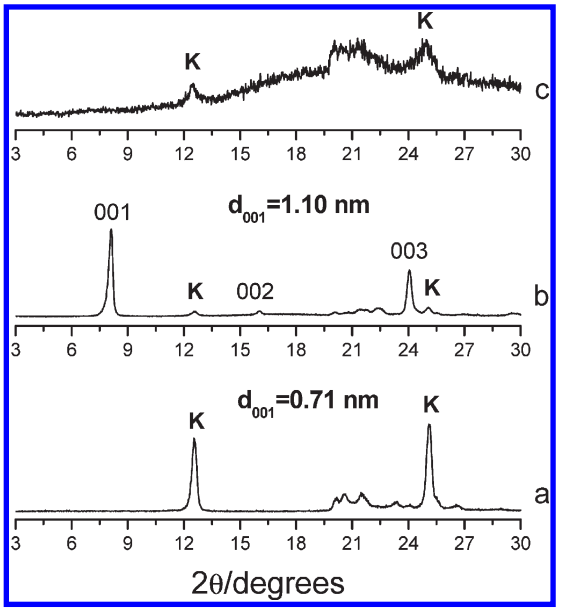

Figure 2. Oriented XRD patterns (2θ = 3−30°) of (a) kaolinite; (b) DMSO-K, and (c) the resulting microcomposite obtained after reaction of DMSO-K with IL_1.

Polymerization−Exfoliation Reaction (Scheme 2). Two grams of the ionic liquid (IL_1, IL_2, or IL_3) was dissolved in 100 mL of isopropyl alcohol. The mixture was heated and stirred at 80 °C. Then, 500 mg of Urea-K or DMSO-K was then added to the mixture (IL/Urea-K w/w = 4/1; IL/DMSO-K w/w = 4/1). The suspension was magnetically stirred at 90 °C overnight under a flow of nitrogen. The molten salt in excess was removed after four series of washing−centrifugation using isopropyl alcohol. The recuperated solid sample was dried at 60 °C overnight, grounded, and stored for further characterization.

Characterization. X-ray diffraction patterns (XRD) were obtained with a Philips PW 3710 instrument equipped with Ni-filtered Cu Kα radiation (λ = 0.15418 nm) operating at 45 kV and 40 mA. Differential thermal analyses (DTA) and thermal gravimetric analyses (TGA) were recorded on a SDT 2960 simultaneous DSC-TGA instrument under N_2 flow (100 mL/min) with a heating rate of 10 °C/min. The ^{1}H and ^{13}C NMR spectra in solution were recorded on a Bruker 400 MHz spectrometer. ^{13}C CP/MAS NMR spectra were collected on a Bruker AVANCE 500 NMR spectrometer operating at 125.77 MHz. The ^{13}C NMR chemical shifts were referenced to TMS at 0 ppm using the high-frequency signal of adamantane at 38.4 ppm as a secondary standard. ^{29}Si CP/MAS NMR spectra were collected on a Bruker AVANCE 500 NMR spectrometer operating at 99.35 MHz. The ^{29}Si NMR chemical shifts were referenced to TMS at 0 ppm using the high-frequency signal of tetrakis(trimethylsilyl)silane at 29.9 ppm as a secondary standard. A SEM microscope JSM-7500F FESEM (JEOL) model, operating at an accelerating voltage of 2 kV, was used for the structural characterization of the modified materials.

RESULTS AND DISCUSSION

XRD. Figure 1 displays powder XRD diffractograms of kaolinite (Figure 1a), the Urea-K intercalate (Figure 1b), and the resulting nanocomposite obtained after reaction with 1-methyl-3-(4-vinylbenzyl)imidazolium chloride (Figure 1c). After intercalation of urea, the 001 reflection shifts to a lower angle due to the expansion of the interlayer space. The d_{001} spacing of Urea-K is close to 1.06 nm, in agreement with previously reported values.[29,45] It corresponds to a d-spacing expansion of 0.35 nm compared to kaolinite. After reaction with the imidazolium salt, one of these situations could be expected:

(i) An increase of the interlayer space due to the displacement of urea and intercalation of the salt (in polymer or monomer form) or also by co-intercalation of the salt with urea. In this case, the 001 reflection would shift at lower angle with respect to the 001 reflection observed in the XRD pattern of Urea-K intercalate (ca. d_{001} = 1.06 nm).

(ii) A displacement of urea from the interlayer space without intercalation of the imidazolium salt. In this case, kaolinite would be recovered, and the 001 reflection would appear at the 001 reflection of kaolinite (ca. d_{001} = 0.71 nm).

(iii) An exfoliation of the individual layers of the clay giving rise to a series of individual sheets randomly oriented without any periodicity.

(iv) A complex system formed by various phases: exfoliated, delaminated, intercalated, and/or recovered kaolinite.

The diffractogram of the compound obtained by reaction with 1-methyl-3-(4-vinylbenzyl)imidazolium chloride showed a disappearance of the 001 reflection at 1.06 nm without recovery of the 001 reflection of kaolinite at 0.71 nm (Figure 1c). This result indicates that the structure of the synthesized nanohybrid material does not present any periodicity along the c axis, at least in the limits of the XRD experiment (above 2θ = 2° (4.42 nm)). This was the indication of the possible formation of an exfoliated nanocomposite. The presence of a well-defined reflection at 2θ = 62.3° (0.149 nm), corresponding to the 060 reflection which is characteristic of a dioctahedral clay mineral, indicated that the structure of kaolinite was not altered in the a,b directions. It was, however, not clear if this possible exfoliation was made by the intercalation of the 1-methyl-3-(4-vinylbenzyl)imidazolium chloride as a monomer followed by exfoliation or rather by a spontaneous polymerization−exfoliation process. This point will be clarified by ^{13}C CP/MAS NMR analysis. The same features were observed for the nanocomposites prepared by reaction of Urea-K with IL_2 and IL_3 (figures not shown).

Figure 2 displays the oriented XRD diffractograms of kaolinite (Figure 2a), the DMSO-K intercalate (Figure 2b), and the

resulting composite obtained after reaction of DMSO-K with 1-methyl-3-(4-vinylbenzyl)imidazolium chloride (Figure 1c). The oriented XRD patterns of the starting DMSO-K preintercalate exhibits well-developed shifted 00*L* reflections (001, 002, and 003) with intense 001 reflection at 1.10 nm corresponding to the insertion of the DMSO molecules in the interlayer spaces of kaolinite. After reaction of DMSO-K with IL_1, the 001 reflection corresponding to DMSO-K disappeared and an increase of the intensity of the 001 reflection corresponding to kaolinite could be observed. This could be interpreted by a partial exfoliation of kaolinite along with a collapse of its structure, resulting in a mixture of kaolinite platelet aggregates with an exfoliated nanocomposite. The d_{060} reflection of kaolinite characteristic of a dioctahedral clay mineral (not shown) remained at 0.149 nm, indicating also that the (*a*,*b*) structure of the layers of kaolinite was largely unaffected during the reaction process. The same features were observed for the composites prepared by reaction of DMSO-K with IL_2 and IL_3 (figures not shown).

TG-DTA. The TG pattern of kaolinite is mainly characterized by one weight loss (13.9%) with a maximum at 514 °C (Figure S1a in Supporting Information) accompanied by an endothermic peak at the same temperature. This is due to the dehydroxylation of kaolinite, corresponding to the transformation of kaolinite $Al_2Si_2O_5(OH)_4$ to metakaolinite $Al_2Si_2O_7$. The thermogram of the Urea-K intercalate exhibits three weight losses with maxima at 53, 210, and 494 °C (Figure S1b). They are accompanied by three endotherms centered, respectively, at 61, 217, and 507 °C. The first loss is due to the removal of water molecules adsorbed on the external surfaces. The second is attributed to the loss and decomposition of urea from the interlayer space of kaolinite, and finally, the third one is due to the dehydroxylation step of kaolinite. The thermogram of DMSO kaolinite intercalate is also characterized by three weight losses with maxima at 65, 181, and 512 °C (Figure S1d). They are accompanied by three endotherms centered, respectively, at 58, 185, and 517 °C. The first loss is due to the removal of molecular water adsorbed on the external surface. The second is attributed to the loss and decomposition of DMSO from the interlayer space of kaolinite, and finally, the third one is due to the dehydroxylation step of kaolinite. TG pattern of the resulting nanocomposite obtained by reaction of Urea-K with 1-methyl-3-(4-vinylbenzyl)imidazolium chloride is given in Figure S1c. The first weight loss observed at 85 °C and accompanied by an endotherm at 98 °C corresponds to the removal of water externally adsorbed. The second loss observed in the range of 150−350 °C is attributed to a partial thermal decomposition of the organic material associated with the clay mineral. This phenomenon is accompanied by a broad endothermic peak centered at 281 °C. Finally, the third loss observed at 438 °C is due to the decomposition of the remaining organic units concurrently with the kaolinite dehydroxylation. The dehydroxylation of the layer sheets occurs at temperatures around 438 °C, well below the dehydroxylation temperature of kaolinite (514 °C). This phenomenon was also observed in the case of the nanohybrid materials prepared by the grafting of amino alcohols[47,48] and also for the nanocomposite obtaining upon exfoliation with polyacrylate[30] and of primary *n*-alkylamines.[31] It is proposed that this is due to the loss of structuration of the kaolinite internal surfaces, the H-bond network linking the aluminol to the siloxane surfaces being lost. In the case of the composite prepared by the reaction of DMSO-K with the ionic liquid, the dehydroxylation of the layers takes place at a similar temperature, 434 °C, but it is accompanied by a second dehydroxylation event at 492 °C. This is an indication of the nature of the resulting composite, a mixture of micro- and nanocomposites. As it was mentioned above, the dehydroxylation of the exfoliated layers occurs at lower temperatures, close to 434 °C, whereas the dehydroxylation of the collapsed layers takes place at 492 °C. From the thermograms, one can evaluate the amount of organic material in the nanocomposite. Directly after reaction, the amount of organic material was in the range of 60−75% of organic material. When the nanocomposite was thoroughly washed, however, by four series of washing−centrifugation using isopropyl alcohol, an amount of organic material as low as 26% could be obtained.

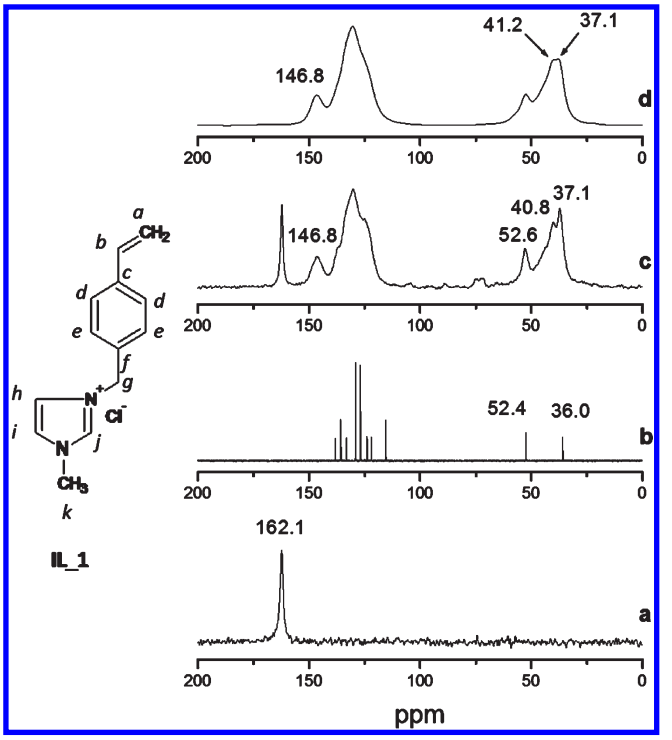

Figure 3. Solid-state ^{13}C CP/MAS NMR spectra of (a) urea-K intercalate; (b) ^{13}C NMR spectrum of IL_1 in solution, given for reference; (c) the resulting exfoliated nanocomposite obtained after the reaction of Urea-K with IL_1; (d) the polymer obtained by polymerization of IL_1.

^{13}C NMR. The ^{13}C CP/MAS NMR spectra of the Urea-K intercalate and of the nanocomposite resulting from its reaction with 1-methyl-3-(4-vinylbenzyl)imidazolium chloride are presented in Figure 3a,c. The Urea-K intercalate (Figure 3a) shows only one peak at 162.1 ppm corresponding to the urea carbonyl group. For comparison, the spectrum of 1-methyl-3-(4-vinylbenzyl)imidazolium (IL_1) in solution is given in the same figure (Figure 3b) as well as the one of the polymer obtained independently by polymerization of the IL_1 in the presence of AIBN (Figure 3d).

The attribution of the peaks of the ^{13}C high-resolution NMR spectrum of IL-1 in D_2O solution (Figure 3b) is described in the Experimental Section. Of particular interest is the peak at 115.6 ppm corresponding to the vinyl β carbon (C_a in our notation). Upon intercalation and reaction of the ionic liquid in kaolinite, this peak disappears (Figure 3c), indicating polymerization of the vinyl group. The chemical shift of the α carbon is 138.2 ppm, too close to the group of aromatic and imidazolium peaks to be diagnostic of the polymerization since the polymer resonances

dx.doi.org/10.1021/la203492m |*Langmuir* 2011, 27, 15248–15254

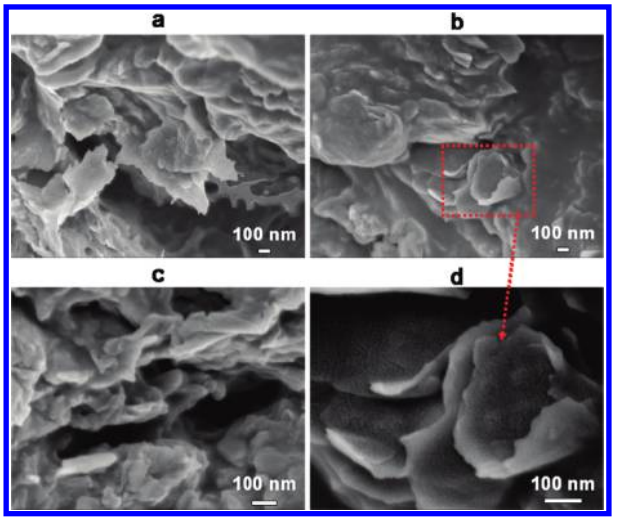

Figure 4. SEM images of the exfoliated nanocomposite obtained by reaction of Urea-K with IL_1: (a,b) 50 000× magnification, (c) 100 000× magnification, and (d) 140 000× magnification.

cover a broad range from 120 to 135 ppm. Two new broad peaks (Figure 3c) appear in the regions of 40−48 ppm, corresponding to the aliphatic backbone of the polymer, and at 146.8 ppm. The latter one is characteristic of polystyrene,[49,50] corresponding to the aromatic *ipso* carbon attached to the backbone (C_c in our notation). Its broadness does not allow a detailed discussion on the tacticity of the polymer, but it suggests the formation of an atactic polystyrene.[49,50] The observation of a relatively sharp peak at 162 ppm indicates that urea was not completely exchanged during the intercalation of IL_1 and the exfoliation. The ^{13}C CP/MAS NMR spectra of the nanocomposite (Figure 3c) and the one of the independently synthesized polymer (Figure 3d) are essentially identical (except for the presence of urea in the nanocomposite).

SEM. The morphology of the KGa-1b kaolinite is illustrated in Figure S2a,b. It is composed of pseudo-hexagonal-shaped platelets that have well-defined edges and corner angles, indicative of a high degree of crystallinity consistent with the XRD data. The crystalline platelets in pure kaolinite form well-ordered stacks. After intercalation with urea or DMSO, the morphology of the resulting Urea-K or DMSO-K intercalates (Figure S2c,d) is markedly different from kaolinite. The platelets are smaller and irregular with no hexagonal symmetry or well-defined edges or corner angles. Furthermore, the height of the stacks is, in general, much smaller in comparison to the stacks in kaolinite, indicating disruption of long-range ordering in Urea-K and DMSO-K intercalates. On the other hand, the observation of small stacks suggests that short-range-ordered structures still pertain. In the nanocomposite, produced from the reaction of Urea-K with IL_1, IL_2, and IL_3, SEM micrographs (Figure 4 and Supporting Information Figure S3 and Figure S4, respectively) reveal individual thin flakes or agglomerated flakes. Some of the flakes are curled up, and some have leaf-like morphology. Figure 4d (highest magnification) shows the formation of curled layers, characteristic of kaolinite exfoliation. The thickness of these layers is in the order of the nanometer, indicating the presence of single layers. There is indication of some stacks, quite expected on the basis of the amount of mineral material in the polymer. These results indicate that exfoliation of the individual platelet layers has occurred in the nanocomposite. In contrast, in the case

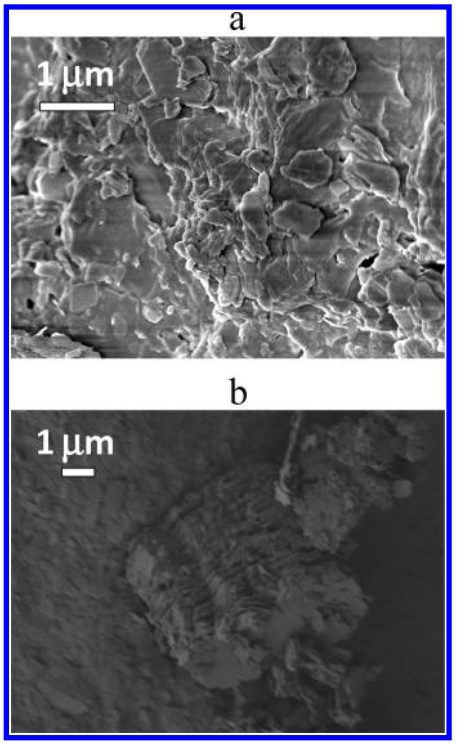

Figure 5. SEM images of the aggregated microcomposite obtained by reaction of DMSO-K with (a) IL_1 (9000× magnification) and (b) IL_2 (20 000× magnification).

of the composites prepared by reaction of the DMSO-K preintercalate with IL_1, IL_2, and IL_3, SEM micrographs indicate that the morphology of these samples is not homogeneous. The SEM micrographs of some areas are identical to those of pure kaolinite (Figure 5b). In other areas, the platelets are separated but not folded like in the case of the nanocomposite obtained using Urea-K as the starting material (Figure 5a). The SEM results, together with the XRD results, point to the conclusion that a complete exfoliation of the kaolinite layers took place when the reaction was done using Urea-K as a preintercalate, resulting in the formation of an exfoliated nanocomposite, whereas only a partial separation of the platelets occurred when the reaction was done using DMSO-K as the precursor, resulting in a mixture of some exfoliated nanocomposites with a microcomposite phase.

The presence of a bulky polymer inside the interlayer spaces of kaolinite results in an increase of the distance between the layer sheets and in a reduction of the interactions between them, leading to a complete loss of layer−layer interactions and the random dispersion of the individual layers in the polymeric matrix.

The exfoliation can be achieved when the release of the preintercalated molecule and the intercalation of the monomer occur simultaneously. If the release occurs before a possible intercalation of the monomer, a collapse of the structure results, with the recovery of kaolinite that becomes dispersed in the polymer to form a microcomposite.

CONCLUSION

Exfoliated nanocomposites of kaolinite could be obtained by the intercalation and polymerization of ionic liquids in a urea kaolinite preintercalate. The morphology of the obtained

nanocomposite consisted of individual exfoliated layers of kaolinite dispersed in a continuous mixture of polymer and some remaining urea. The same approach was used with a DMSO kaolinite intercalate as starting material. In this case, the resulting composite was a mixture of partially exfoliated individual layers of kaolinite and collapsed ones. The choice of the nature of the starting preintercalate of kaolinite is crucial for the nature of the resulting composite, nano or micro. The choice of an ionic liquid monomer is also crucial because it allowed the one-step process of intercalation/polymerization/exfoliation. By an appropriate treatment of the nanocomposite, the amount of organic material could be close to 30%, giving a nanocomposite with a high inorganic content.

With internal surfaces covered by aluminol groups that can be used for further functionalization,[51,52] the layers of kaolinite have properties highly different from those of the smectites, which are largely used in the making of nanocomposites. The possibility of creating exfoliated nanocomposites based on kaolinite, in a simple one-step polymerization−exfoliation process, opens the way to the design of exfoliated nanocomposites where organic polymer and inorganic alumino silicate layers are covalently bound in a structurally controlled approach. In contrast with the case of smectites, the degree of swelling of kaolinite in these nanocomposites cannot yet be controlled nor can the formation of oriented films. This is a goal for future work.

■ ASSOCIATED CONTENT

Supporting Information. Additional figures. This material is available free of charge via the Internet at http://pubs.acs.org.

■ AUTHOR INFORMATION

Corresponding Author
*E-mail: dete@uottawa.ca.

■ ACKNOWLEDGMENT

This work was financially supported by a Discovery Grant of the Natural Sciences and Engineering Research Council of Canada (NSERC). The Canada Foundation for Innovation and the Ontario Research Fund are gratefully acknowledged for infrastructure grants to the Center for Catalysis Research and Innovation of the University of Ottawa. Dr. Glenn A. Facey is thanked for recording some of the NMR spectra.

■ REFERENCES

(1) *Functional Hybrid Materials*; Gómez-Romero, P.; Sanchez, C., Eds.; Wiley-VCH: Weinheim, Germany, 2004.
(2) Bergaya, F.; Jaber, M.; Lambert, J. F. Clays and Clay Minerals. In *Rubber-Clay Nanocomposites: Science, Technology, and Applications*; Galimberti, M., Ed.; Wiley: New York, 2012; in press, Chapter 1.
(3) Hsu, H. L.; Jehng, J. M.; Liu, Y. C. *Mater. Chem. Phys.* **2009**, *113*, 166–171.
(4) Shim, B. S.; Tang, Z.; Morabito, M. P.; Agarwal, A.; Hong, H.; Kotov, N. A. *Chem. Mater.* **2007**, *19*, 5467–5474.
(5) Kiersnowski, A.; Serwadczak, M.; Kulaga, E.; Futoma-Koloch, B.; Bugla-Ploskonska, G.; Kwiatkowski, R.; Doroszkiewicz, W.; Piglowski, J. *Appl. Clay Sci.* **2009**, *44*, 225–229.
(6) Katti, D. R.; Ghosh, P.; Schmidt, S.; Katti, K. S. *Biomacromolecules* **2005**, *6*, 3276–3282.
(7) Peeterbroeck, S.; Lepoittevin, B.; Pollet, E.; Benali, S.; Broekaert, C.; Alexandre, M.; Bonduel, D.; Viville, P.; Lazzaroni, R.; Dubois, P. *Polym. Eng. Sci.* **2006**, *46*, 1022–1030.
(8) Yang, H.; Wilson, M.; Fairbridge, C.; Ring, Z.; Hill, J. M. *Energy Fuels* **2002**, *16*, 855–863.
(9) Han, Y.; Lu, Y. *J. Appl. Polym. Sci.* **2009**, *111*, 2400–2407.
(10) Zhang, X; Yang, W.; Ma, Y. *Electrochem. Solid-State Lett.* **2009**, *12*, A95–A98.
(11) Liu, L.; Grunlan, J. C. *Adv. Funct. Mater.* **2007**, *17*, 2343–2348.
(12) Monticelli, O.; Bottino, A.; Scandale, I.; Capannelli, G.; Russo, S. *J. Appl. Polym. Sci.* **2007**, *103*, 3637–3644.
(13) Thomassin, J. M.; Pagnoulle, C.; Caldarella, G.; Germain, A.; Jerome, R. *J. Membr. Sci.* **2006**, *270*, 50–56.
(14) Song, M. K.; Park, S. B.; Kim, Y. T.; Rhee, H. W.; Kim, J. *Mol. Cryst. Liq. Cryst.* **2003**, *407*, 411–419.
(15) Letaief, S.; Martin-Luengo, M. A.; Aranda, P.; Ruiz-Hitzky, E. *Adv. Funct. Mater.* **2006**, *16*, 401–409.
(16) Manova, E.; Aranda, P.; Martín-Luengo, M. A.; Letaief, S.; Ruiz-Hitzky, E. *Microporous Mesoporous Mater.* **2010**, *131*, 252–260.
(17) (a) Osada, Mi.; Sasaki, T. *J. Mater. Chem.* **2009**, *19*, 2503–2511. (b) Ma, R.; Sasaki, T. *Adv. Mater.* **2010**, *22*, 5082–5104.
(18) (a) Alberti, G.; Casciola, M.; Costantino, U. *J. Colloid Interface Sci.* **1985**, *107*, 256–263. (b) Yamamoto, N.; Okuhara, T.; Nakato, T. *J. Mater. Chem.* **2001**, *11*, 1858–1863. (c) Bissessur, R.; MacDonald, J. *Mater. Chem. Phys.* **2007**, *106*, 256–259.
(19) (a) Nazar, L. F.; Liblong, S. W.; Yin, X. T. *J. Am. Chem. Soc.* **1991**, *113*, 5889–5890. (b) Schaak, R. E.; Mallouk, T. E. *Chem. Mater.* **2002**, *14*, 1455–1471. (c) Fuse, Y.; Ide, Y.; Ogawa, M. *Polym. Chem.* **2010**, *1*, 849–853.
(20) (a) Leroux, F.; Adachi-Pagano, M.; Intissar, M.; Chauvière, S.; Forano, C.; Besse, J. P. *J. Mater. Chem.* **2001**, *11*, 105–112. (b) Hibino, T. *Chem. Mater.* **2004**, *16*, 5482–5488. (c) Liu, Z.; Ma, R.; Ebina, Y.; Iyi, N.; Takada, K.; Sasaki, T. *Langmuir* **2007**, *23*, 861–867. (d) McIntyre, L. J.; Jackson, L. K.; Fogg, A. M. *Chem. Mater.* **2008**, *20*, 335–340. (e) Yoon, Y. S.; Lee, B. I.; Lee, K. S.; Im, G. H.; Byeon, S. H.; Lee, J. H.; Lee, I. S. *Adv. Funct. Mater.* **2009**, *19*, 3375–3380.
(21) (a) Takahashi, N.; Kuroda, K. *J. Mater. Chem.* **2011**, *21*, 14336–14353. (b) Takahashi, N.; Hata, H.; Kuroda, K. *Chem. Mater.* **2011**, *23*, 266–273. (c) Takahashi, N.; Hata, H.; Kuroda, K. *Chem. Mater.* **2010**, *22*, 3340–3348. (d) Isoda, K.; Kuroda, K.; Ogawa, M. *Chem. Mater.* **2000**, *12*, 1702–1707.
(22) Bergaya., F.; Theng, B. K. G.; Lagaly, G., Eds. *Handbook of Clay Science*; Elsevier Ltd.: Amsterdam, 2006.
(23) Lim, S. H.; Yu, Z. Z.; Mai, Y. W. *Adv. Mater. Res.* **2008**, *47−50*, 694–697.
(24) Treece, M. A.; Oberhauser, J. P. *Polymer* **2007**, *48*, 1083–1095.
(25) Galimberti, M.; Lostritto, A.; Spatola, A.; Guerra, G. *Chem. Mater.* **2007**, *19*, 2495–2499.
(26) Liu, G.; Zhang, L.; Zhao, D.; Qu, X. *J. Appl. Polym. Sci.* **2005**, *96*, 1146–1152.
(27) Gam, K. T.; Miyamoto, M.; Nishimura, R.; Sue, H. J. *Polym. Eng. Sci.* **2003**, *43*, 1635–1645.
(28) Letaief, S.; Ruiz-Hitzky, E. *Chem. Commun.* **2003**, *24*, 2996–2997.
(29) Wang, M. S.; Pinnavaia, T. J. *Chem. Mater.* **1994**, *6*, 468–474.
(30) Letaief, S.; Detellier, C. *Langmuir* **2009**, *25*, 10975–10979.
(31) Gardolinski, J. E. F. C.; Lagaly, G. *Clay Miner.* **2005**, *40*, 547–556.
(32) (a) Kuroda, Y.; Ito, K.; Itabashi, K.; Kuroda, K. *Langmuir* **2011**, *27*, 2028–2035. (b) Matusik, J.; Wisla-Walsh, E.; Gawel, A.; Bielanska, E.; Bahranowski, K. *Clays Clay Miner.* **2011**, *59*, 116–135. (c) Matusik, J.; Gawel, A.; Bielanska, E.; Oshuch, W.; Bahranowski, K. *Clays Clay Miner.* **2009**, *57*, 452–464.
(33) *Hydrous Phyllosilicates*; Bailey, S. W., Ed.; American Mineralogical Society: Washington, DC, 1988.
(34) Newman, A. C. D.; Brown, G. The Chemical Constitution of Clays. In *Chemistry of Clays and Clay Minerals*; Newman, A. C. D., Ed.; Longman Scientific and Technical. Monograph, n6. Mineralogical Society: London, 1987; Chapter 1.
(35) Elbokl, T. A.; Detellier, C. *Can. J. Chem.* **2009**, *87*, 272–279.
(36) Essawy, H. A.; Youssef, A. M.; Abd El-Hakim, A. A.; Rabie, A. M. *Polym. Plast. Technol. Eng.* **2009**, *48*, 177–184.

(37) Zhang, B.; Li, Y.; Pan, X.; Jia, X.; Wang, X. *J. Phys. Chem. Solids* **2007**, *68*, 135–142.
(38) Cabedo, L.; Gimenez, E.; Lagaron, J. M.; Gavara, R.; Saura, J. J. *Polymer* **2004**, *45*, 5233–5238.
(39) Itagaki, T.; Komori, Y.; Sugahara, Y.; Kuroda, K. *J. Mater. Chem.* **2001**, *11*, 3291–3295.
(40) Gardolinski, J. E.; Carrera, L. C. M.; Cantao, M. P.; Wypych, F. *J. Mater. Sci.* **2000**, *35*, 3113–3119.
(41) Komori, Y.; Sugahara, Y.; Kuroda, K. *Chem. Mater.* **1999**, *11*, 3–6.
(42) Tunney, J. J.; Detellier, C. *Chem. Mater.* **1996**, *8*, 927–935.
(43) Sugahara, Y.; Satokawa, S.; Kuroda, K.; Kato, C. *Clays Clay Miner.* **1988**, *36*, 343–348.
(44) Letaief, S.; Detellier, C. *J. Mater. Chem.* **2005**, *15*, 4734–4740.
(45) Letaief, S.; Elbokl, T. A.; Detellier, C. *J. Colloid Interface Sci.* **2006**, *302*, 254–258.
(46) Zhao, D.; Fei, Z.; Ang, W. H.; Dyson, P. J. *Small* **2006**, *2*, 879–883.
(47) Brandt, K. B.; Elbokl, T. A.; Detellier, C. *J. Mater. Chem.* **2003**, *13*, 2566–2572.
(48) Letaief, S.; Detellier, C. *J. Therm. Anal. Calorim.* **2011**, *104*, 831–839.
(49) Wang, Y.-Y.; Li, B.-X.; Zhu, F.-M.; Gao, H.-Y.; Wu, Q. *J. Appl. Polym. Sci.* **2011**, *122*, 545–550.
(50) Yu, S.; He, X.; Chen, Y.; Liu, Y.; Hong, S.; Wu, Q. *J. Appl. Polym. Sci.* **2007**, *105*, 500–509.
(51) Letaief, S.; Detellier, C. *Chem. Commun.* **2007**, 2613–2615.
(52) Hirsemann, D.; Köster, T. K.-J.; Wack, J.; van Wüllen, L.; Breu, J.; Senker, J. *Chem. Mater.* **2011**, *23*, 3152–3158.